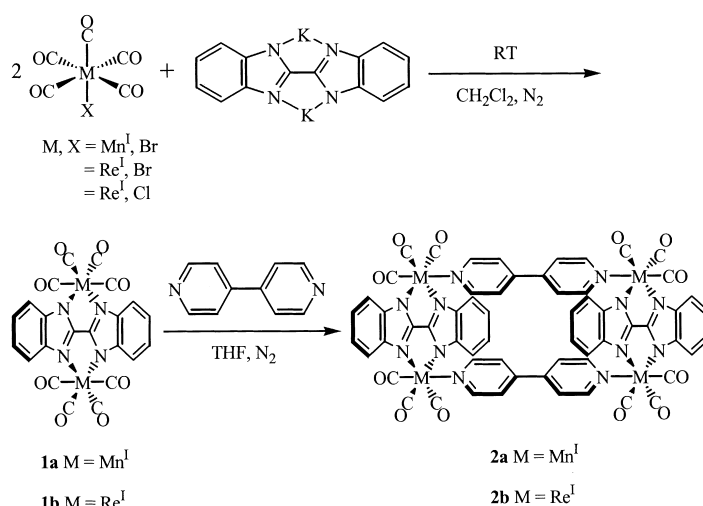# Luminescent Mesoporous Molecular Materials Based on Neutral Tetrametallic Rectangles**

Kurt D. Benkstein, Joseph T. Hupp,* and
Charlotte L. Stern

There has been tremendous recent interest in the synthesis of discrete inorganic and organometallic cyclophanes as candidate host species for selective guest binding.[1–7] We have previously reported on tetrametallic square cyclophanes, which function in the solid state as sensors for volatile organic compounds (VOCs) or as molecular sieves, and on other materials which behave as luminescent sensors for anions in solution.[8, 9] Reasoning that a rectangular cavity would offer enhanced binding and selectivity for, for example, planar aromatic guest species, we sought to develop useful transition metal based "molecular rectangles".[10–12] While the first rectangles we made were either too small to accommodate guests or carried an undesired charge, they did give us insight into a synthetic strategy for the formation of mixed-ligand metallocyclophanes. (The charged compounds are of little value as building blocks for mesoporous materials because counterions block the channels formed by cavities; furthermore, because of their charge, the compounds are slightly water soluble, which precludes their use in aqueous environments.) Using a similar method, we developed a new family of metal-based molecular rectangles, that use a rigid, dianionic bisbenzimidazolate bridge—both to compensate for the cationic metal charge and to provide a cavity wide enough to serve as a host for small, planar, aromatic guest compounds.

The molecular rectangles were synthesized according to Scheme 1. The absence of long-chain oligomers, as opposed to macrocycles, was initially indicated by a) ¹H NMR spectroscopy, which showed only well resolved signals for each of the protons, b) FAB mass spectrometry, which showed no significant peaks at higher m/z ratios, and c) its high solubility product in several polar organic solvents (such as THF, $CHCl_3$, CH_2Cl_2, and acetone, but not in short-chain alcohols, CH_3CN, and hexanes).

Single-crystal X-ray diffraction (XRD) studies of **2a** yielded the ORTEP representation shown in Figure 1.[13] The dimensions of the cavity, as defined by the Mn atoms, are 11.2×5.5 Å. However, the 4,4′-bipyridine (4,4′-bpy) bridges are bowed inward (presumably a packing effect), such that the cavity width at the center is only 3.9 Å. A similar

[*] Prof. J. T. Hupp, K. D. Benkstein, C. L. Stern
Department of Chemistry and Center for Nanofabrication and Molecular Self Assembly
Northwestern University
2145 Sheridan Road, Evanston, IL 60208-3113 (USA)
Fax: (+1) 847-491-7713
E-mail: jthupp@chem.nwu.edu

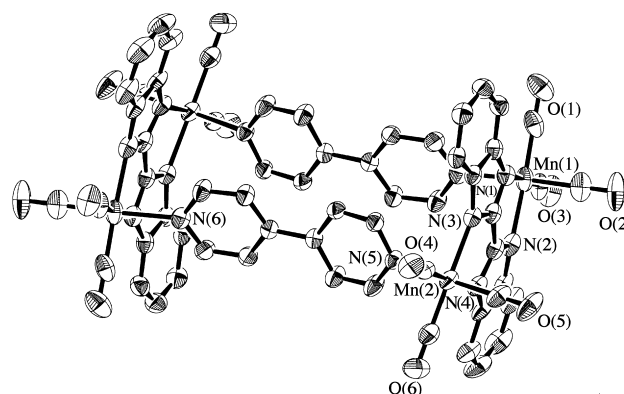Scheme 1. Synthesis of bisbenzimidazolate-derived molecular rectangles.

Figure 1. An ORTEP representation of **2a**, that shows a rectangular cavity of dimensions 11.2×5.5 Å, as defined by the metal atoms. For clarity, the hydrogen atoms have been omitted. Two THF molecules and a disordered THF/hexane site are also present in the unit cell but are not shown. The thermal ellipsoids represent 50 % occupancy.

structure, based on $[\{(CO)_3Re\}_2(\text{bipyrimidine})]^{2+}$ edges, previously yielded a cavity measuring 11.6×5.9 Å, without bowing.[10b] The packing diagram (Figure 2) shows that a) the intramolecular cavity *openings* of all the molecules are similarly aligned and b) *intermolecular* vacancies (roughly rectangular), of nearly the same size ($\sim 10 \times 6$ Å), also exist—effectively doubling the number of sites potentially available for the uptake of guest molecules. From this diagram, both the intra- and the intermolecular effective cavity volumes are estimated to be about 600 Å³.

The UV/Vis absorption spectrum of **2b** shows a band in the high energy region of the visible region, which is absent in **1b**. We ascribe the extra band to an allowed Re ↔ bpy singlet charge transfer. Unlike either **2a** or the bipyrimidine-edged rectangle,[10b] **2b** luminesces in both the solution (for example, $\lambda_{max}(\text{THF}) = 617$ nm) and the solid state ($\lambda_{max} = 572$ nm). The emission lifetime τ varies with the (deoxygenated) solvent: $\tau(CHCl_3) = 238$ ns but $\tau(\text{THF/MeOH}) = \tau(\text{THF/MeOD}) = 26$ ns. The comparatively long lifetimes and substantial emission Stokes shifts suggest the emission occurs from a predominantly triplet charge-transfer state, or states. The emission in solution is rapidly quenched dynamically by
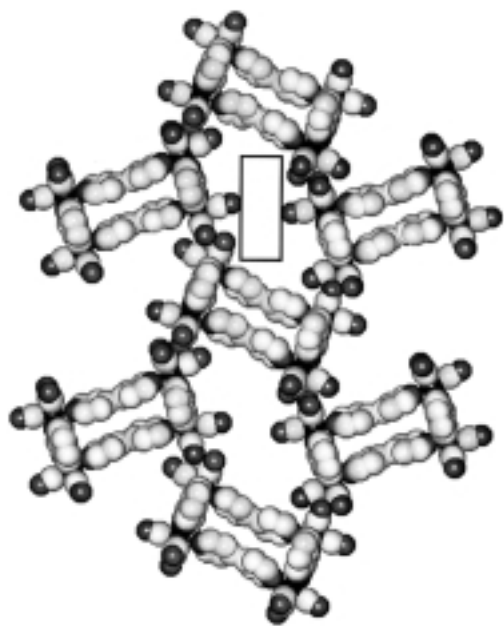
Figure 2. A space-filling model representation of a portion of the unit cell of **2a**, to show intra- and intermolecular (drawn box) cavities. For clarity, the solvent molecules have not been shown.
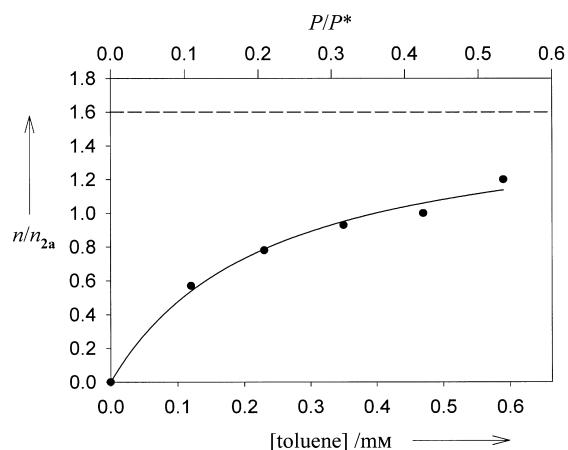

Figure 3. QCM-derived affinity data and best fit (solid line) for toluene uptake by a thin film of **2a**. The films were placed in vacuum for a minimum of eight hours prior to the measurement to remove encapsulated solvent molecules. The y axis shows the molar ratio of adsorbed guest toluene (n) to host **2a** (n_{2a}) in the film. From the fit line, the limiting host to guest ratio is ~ 1.6 (dashed line). For reference, the top axis provides the absolute pressure of toluene ($P =$ pressure of toluene in the chamber; $P^* =$ saturation vapor pressure of toluene at $24\,^{\circ}$C).

Table 1. Affinities of thin films of **2a** and a representative "molecular square" towards selected VOCs.

VOC	**2a** [M^{-1}]	$[Re(CO)_3Cl(\eta\text{-pyrazine})]_4$ [M^{-1}][a]
toluene	3200 ± 1900	332 ± 26
4-fluorotoluene	1400 ± 360	200 ± 42
benzene	740 ± 250[b]	157 ± 8
fluorobenzene	420 ± 80	87 ± 8
hexafluorobenzene	460 ± 110	47 ± 8

[a] From ref. [9]. [b] Value for **2b** is $580 \pm 220\,M^{-1}$.

known reductants, such as hydroquinone and *p*-toluidine, which indicates diffusion-controlled, rather than binding, interactions. (Given the τ values, however, binding with an association constant of less than about $50\,M^{-1}$ would be difficult to detect in this way.) The emission of evaporatively cast, solid, thin films of **2b** is similarly quenched upon exposure to *p*-toluidine vapor but enhanced by approximately 50 % and shifted to higher energy upon exposure to THF vapor. The THF exposure also increases τ_{film} from ~ 620 ns to ~ 950 ns. This effect is reversible: After placing a film previously exposed to THF vapor under vacuum for several hours, the luminescent lifetime is again measured to be 620 ns.

Both the film-based emission studies and the crystal structure suggested that, as molecular solids, the rectangles might behave as high internal-surface area, mesoporous host materials. Quantitative assessments of the host behavior of **2a** toward selected VOCs as guests were obtained by quartz crystal microgravimetry (QCM) measurements.[9, 14] These studies showed the following points. a) Film binding capacity is proportional to film thickness, as expected if guest uptake is based on permeation of the film interior rather than simple adsorption to the film exterior. b) At a sufficiently high aryl (guest) concentration (vapor pressure), the guest:host stoichiometry can exceed unity, with a hypothetical limiting ratio between 1:1 to 2:1 implied by fits to affinity curves (see Figure 3; for simplicity, curves were fit by assuming identical affinity constants for the uptake of the first and second guests). The high stoichiometry would seem to suggest that multiple sites are occupied by guest molecules, namely, both intra- and intermolecular cavities are being filled. c) Host – guest affinity constants can depend significantly on the peripheral composition of the aromatic guest (Table 1). Electron-withdrawing substituents diminish the affinity constant, whereas electron-donating substituents enhance it; this could suggest a significant role for electron donor/acceptor (guest/host) interactions in inducing guest uptake. d) Affinity constants for planar aromatic guests are five- to ten-fold greater for the rectangle-based host material **2a** than for a closely related, square-based host material (Table 1). e) Within experimental error, replacement of Mn (**2a**) by Re (**2b**) does not change the affinity constants.

By analogy to N_2 uptake by zeolites and related non-molecular mesoporous materials, the available data for aromatic guest uptake by the solids based on the molecular rectangle can also be used to determine the effective internal surface areas. For example, a BET analysis of the QCM data for benzene uptake by **2a** yields internal surface areas of about $120\ m^2 g^{-1}$ ($1.6 \times 10^5\ m^2 mol^{-1}$, $150\ m^2 mL^{-1}$), in which the area of only one face of the guest molecule has been used. If the probable encapsulating nature of the host – guest interaction is recognized (that is, both faces and portions of the edge of the guest molecule are in contact with the walls of the host cavity), the calculated internal surface area would be roughly doubled.

To conclude, a new family of molecular rectangles has been synthesized and characterized. The new family offers significant advantages over earlier metal-based rectangular host systems including a) overall charge neutrality, which facilitates solid state applications since potentially cavity-filling counterions are absent, b) luminescence, which provides a tag

for sensory applications, and c) the incorporation of Mn into a cyclophane framework, which provides a more economical building block than Re for nonluminescent applications.

Experimental Section

Bimetallic [{(CO)$_4$M}$_2$BiBzIm] edges[15] (BzIm = benzimidazolate) were formed by stirring [M(CO)$_5$X] (M, X = Mn, Br or Re, Cl) with K$_2$[BiBzIm][16, 17] at ambient temperature in CH$_2$Cl$_2$. At the reaction endpoint (monitored by FTIR), the solvent was partially removed and the desired [{(CO)$_4$M}$_2$BiBzIm] product precipitated as a yellow (**1a**) or white (**1b**) powder by addition of Et$_2$O (45% yield).[18] Rectangular cycles were obtained by reacting equimolar amounts of the bimetallic edge with 4,4′-bpy in refluxing THF for two days. Hexanes were added to the flask after cooling to room temperature. Further cooling provided orange-yellow crystals (**2a**) or a bright yellow powder (**2b**) at ~70% yield.[19, 20] Thin films of **2a** and **2b** were cast evaporatively from filtered THF/CHCl$_3$ (1/1) solutions.

Crystallographic data (excluding structure factors) for the structure reported in this paper have been deposited with the Cambridge Crystallographic Data Centre as supplementary publication no. CCDC-139036. Copies of the data can be obtained free of charge on application to CCDC, 12 Union Road, Cambridge CB21EZ, UK (fax: (+44) 1223-336-033; e-mail: deposit@ccdc.cam.ac.uk).

The UV/Vis absorption spectra of **1b** and **2b** are found in the Supporting Information.

[1] M. Fujita, K. Ogura, *Bull. Chem. Soc. Jpn.* **1996**, *69*, 1471, and references therein.

[2] P. J. Stang, B. Olenyuk, *Acc. Chem. Res.* **1997**, *30*, 502, and references therein.

[3] W.-H. Leung, J. Y. K. Cheng, T. S. M. Hun, C.-M. Che, W.-T. Wong, K.-K. Cheung, *Organometallics* **1996**, *15*, 1497.

[4] H. A. Cruse, N. E. Leadbeater, *Inorg. Chem.* **1999**, *38*, 4149.

[5] S.-S. Sun, A. J. Lees, *Inorg. Chem.* **1999**, *38*, 4181.

[6] S. M. Woessner, J. B. Helms, J. F. Houlis, B. P. Sullivan, *Inorg. Chem.* **1999**, *38*, 4380.

[7] R. V. Slone, K. D. Benkstein, S. Bélanger, J. T. Hupp, I. A. Guzei, A. L. Rheingold, *Coord. Chem. Rev.* **1998**, *171*, 221, and references therein.

[8] R. V. Slone, D. I. Yoon, R. M. Calhoun, J. T. Hupp, *J. Am. Chem. Soc.* **1995**, *117*, 11813.

[9] For the experimental setup, see: M. H. Keefe, R. V. Slone, J. T. Hupp, K. F. Czaplewski, R. Q. Snurr, *Langmuir* **2000**, in press.

[10] a) K. D. Benkstein, J. T. Hupp, C. L. Stern, *Inorg. Chem.* **1998**, *37*, 5404; b) K. D. Benkstein, J. T. Hupp, C. L. Stern, *J. Am. Chem. Soc.* **1998**, *120*, 12982.

[11] See also: S. M. Woessner, J. B. Helms, Y. Shen, B. P. Sullivan, *Inorg. Chem.* **1998**, *37*, 5406.

[12] Charged, fluxionally rectangular *organic* cyclophanes are known, see: B. Odell, M. V. Reddington, A. M. Z. Slawin, N. Spencer, J. F. Stoddart, D. J. Williams, *Angew. Chem.* **1988**, *100*, 1605; *Angew. Chem. Int. Ed. Engl.* **1988**, *27*, 1547.

[13] Crystal data for **2a**: crystal dimensions $0.5 \times 0.4 \times 0.2$ mm; monoclinic; space group $P2_1/n$ (No. 14); $a = 16.501(1)$, $b = 20.195(1)$, $c = 13.587(1)$ Å, $\beta = 102.864(1)°$, $V = 4414.1(5)$ Å^3; $Z = 2$; $\rho_{calc} = 1.316$ g cm^{-3}; $2\theta_{max} = 69.5°$; Mo$_{K\alpha}$ radiation, $\lambda = 0.7107$ Å; scan mode ω; $T = 153$ K; 40889 reflections, of which 10900 are unique, and of which 6063 were included in the refinement; data corrected for Lorentz polarization effects; solution by direct methods (SIR92 A. Altomare, M. Cascarano, C. Giacovazzo, A. Guagliardi, *J. Appl. Cryst.* **1993**, *26*, 343) and refinement on $|F^2|$ by full-matrix least-squares procedures (TeXsan for Windows v1.03, Molecular Structure Corporation, Texas, USA); 535 parameters; isotropic refinement of disordered solvent atoms, the remaining nonhydrogen atoms were refined anisotropically; H atoms were included, except in disordered solvent molecules, but not refined; final values $R|F| = 0.059$, $R_w|F| = 0.090$.

[14] G. Z. Sauerbrey, *Physica* **1959**, *155*, 206.

[15] R. Uson, J. Gimeno, *J. Organomet. Chem.* **1981**, *220*, 173.

[16] M. C. Rezende, C. A. Marques, E. L. Dall'Oglio, C. Zucco, *Liebigs Ann.* **1997**, 925.

[17] M. P. Gamasa, E. Garcia, J. Gimeno, C. J. Ballesteros, *Organomet. Chem.* **1986**, *307*, 39.

[18] **1b**: ^{1}H NMR (300 MHz, CDCl$_3$): $\delta = 7.67$ (q, $J = 3$ Hz, 4H), 7.42 (q, $J = 3$ Hz, 4H). FTIR (CH$_2$Cl$_2$): $\tilde{\nu} = 2113$ (w; CO), 2019, 1989, 1949 cm^{-1}. LR-MS: **1b** · 2CO: calcd: $m/z = 772.7$; found: 773.0. Elemental analysis: calcd: C 31.88, H 0.92, N 6.76; found: C 31.66, H 0.97, N 6.50.

[19] **2a**: ^{1}H NMR (300 MHz, [D$_6$]acetone): $\delta = 8.02$ (d, $J = 7$ Hz, 8H), 7.92 (q, $J = 3$ Hz, 8H), 7.42 (q, $J = 2$ Hz, 8H), 7.20 (d, $J = 7$ Hz, 8H). FTIR (THF): $\tilde{\nu} = 2031$ (sh; CO), 2029, 1940, 1919 cm^{-1}. FAB-MS: calcd: $m/z = 1332.7$; found: 1332.3. Elemental analysis: calcd: C 54.07, H 2.42, N 12.61; found: C 53.39, H 3.00, N 12.67. Cyclic voltammetry: reversible reductions (versus ferrocene): -1.76 V (bpy$^{-/0}$/bpy^0), -1.97 V (bpy$^-$/bpy$^{-/0}$), -2.42 V (multielectron wave).

[20] **2b**: ^{1}H NMR (500 MHz, CDCl$_3$): $\delta = 8.13$ (d, $J = 6$ Hz, 8H), 7.83 (q, $J = 3$ Hz, 8H), 7.43 (q, $J = 3$ Hz, 8H), 6.77 (d, $J = 6$ Hz, 8H). FTIR (THF): $\tilde{\nu} = 2026$ (sh; CO), 2023, 1921, 1908 cm^{-1}. FAB-MS: calcd: $m/z = 1857.8$; found: 1858.1. Elemental analysis (**2b** · 1 THF): calcd: C 39.83, H 2.09, N 8.71; found: C 39.50, H 2.44, N 8.12. Cyclic voltammetry: reversible reductions (versus ferrocene): -1.47 V (bpy$^{-/0}$/bpy^0), -1.70 V (bpy$^-$/bpy$^{-/0}$), -2.28 V, -2.43 V.

Enantioselective Synthesis of 4-Unsubstituted 3-Alkoxy- and 3-Aminoazetidin-2-ones from Formaldehyde *N,N*-Dialkylhydrazones**

Rosario Fernández, Ana Ferrete, José M. Lassaletta,* José M. Llera,* and Angeles Monge

The presence of the azetidin-2-one ring in several widely used families of antibiotics, which include the penicillins and carbapenems, has stimulated considerable activity directed at the stereocontrolled synthesis of β-lactams.[1] One of the most popular methods is the [2+2] cycloaddition reaction of ketenes to imines (the Staudinger reaction).[2] The particular

[*] Dr. J. M. Lassaletta
Instituto de Investigaciones Químicas (CSIC-USe)
c/ Americo Vespuccio s/n, Isla de la Cartuja
41092 Sevilla (Spain)
Fax: (+34) 95-446-0565
E-mail: jmlassa@cica.es

Dr. J. M. Llera
Dpto. de Química Orgánica y Farmacéutica
Universidad de Sevilla
41081 Sevilla (Spain)
Fax: (+34) 954 233 765
E-mail: llera@fafar.us.es

Dr. R. Fernández, A. Ferrete
Dpto. de Química Orgánica
Universidad de Sevilla, Seville (Spain)

Dr. A. Monge
Instituto de Ciencia de Materiales de Madrid, CSIC
Madrid (Spain)